JOURNAL OF AIRCRAFT
Vol. 29, No. 4, July–Aug. 1992

Remote Measurements of Supercooled Integrated Liquid Water During WISP/FAA Aircraft Icing Program

B. B. Stankov,* E. R. Westwater,* J. B. Snider,* and R. L. Weber*
National Oceanic and Atmospheric Administration/Environmental Research Laboratories, Boulder, Colorado 80303

During February and March 1990, the National Center for Atmospheric Research, National Oceanic and Atmospheric Administration (NOAA) Wave Propagation Laboratory, and NOAA Forecast Systems Laboratory conducted the Winter Icing and Storms Project (WISP). Arrays of microwave radiometers, infrared radiometers, lidar ceilometers, radio acoustic sounding systems, and wind profilers were used to determine spatial and temporal distribution of supercooled liquid water. Results are presented from three representative cases to demonstrate that the integrated system that comprises a microwave water substance radiometer, a radio acoustic sounding system, and a ceilometer can identify supercooled liquid water, and that the integrated system that comprises the high resolution wind profiler and the radio acoustic sounding system can identify the distribution of turbulent air pockets within the aircraft icing cloud.

I. Introduction

IT has been known for nearly 20 years that dual-channel microwave radiometers can measure the integrated amount of liquid in a nonprecipitating cloud.[1] Because the response of microwave radiometers to ice clouds is negligibly small, an observed signal is due to liquid alone. This is in sharp contrast to radar, which responds to both liquid and ice phases. Consequently, microwave radiometers were constructed[2] and operated in several experiments designed to augment winter snowfall by seeding supercooled water clouds.[3–5] In these experiments, the radiometers were placed at altitudes above the freezing level so that any liquid measured by the radiometers would be supercooled. In addition, if liquid precipitation were present at the radiometer site, it could be identified by personnel operating the equipment.

Starting in 1980, both a 915-MHz wind profiler and a six-channel microwave radiometer were deployed by the Wave Propagation Laboratory (WPL) at Stapleton International Airport, Denver, Colorado.[6] Using data primarily from the dual-channel portion of the radiometer, Hogg et al.[7] report on observations of liquid and simultaneous reports by pilots (PIREPS) of aircraft icing. Since the surface temperature was below 0°C, the observed liquid was assumed to be supercooled. These initial observations were followed by an in-depth study that compared 2 years of radiometer observations of liquid at Stapleton with PIREPS of icing.[8] In spite of the somewhat sketchy nature of the pilot reports, 90% of the reported icing conditions within 10 miles of the radiometer were identified by the radiometric technique. However, the radiometer measures the total liquid within the radiometer beam and intrinsically cannot distinguish between supercooled and non-supercooled liquid.

Two recent developments in equipment technology suggest that an integrated system can measure remotely and from unattended instruments the presence of supercooled liquid water (SLW).[9,10] The first of these is the development by WPL[11] of a radio acoustic sounding system (RASS). This system combines an acoustic source with wind-profiling radars to provide measurements of virtual temperature and the horizontal wind component with a vertical resolution of about 150–300 m. As discussed in Section II, the altitude range of RASS is highly dependent on the operating frequency of the associated wind-profiling radars.[11] The second important development was the installation by the National Weather Service (NWS) of an automated lidar ceilometer at Stapleton International Airport.

As we demonstrate in this paper, the integrated system, which comprises a dual-channel microwave radiometer (microwave water substance radiometer, MWSR), a RASS, and a ceilometer, can unambiguously identify SLW. We also demonstrate that an integrated system of wind profilers and RASS can provide high-resolution Richardson number computation, which can identify locations where mechanical turbulence is an additional hazard to aircraft.

A description of the 1990 Winter Icing and Storms Project (WISP) is given by Rassmussen and Politovich.[12] A principal objective of the program was to determine the utility of unattended microwave radiometers in detecting and providing input to forecasts of, aircraft icing. Two operational MWSRs were in place at Denver and Platteville, Colorado, and a third MWSR was constructed and deployed near Elbert, Colorado. Several years of experience have shown that the Palmer Ridge region, including Elbert, is a site of frequent aircraft icing conditions.

At the beginning of the 1990 WISP field season, WPL provied research data from the 915-MHz RASS at Stapleton and from a 49.8-MHz RASS at Platteville. During the course of the experiment, data from an experimental 404.37-MHz system at Erie, Colorado, also became available. Real-time measurements from the NWS ceilometer at Stapleton were also acquired by WPL. Wind profiler data, obtained routinely by WPL at the above RASS sites, were also provided to WISP experimenters.

This paper presents the WPL data collected during 3 of 10 representative cases of the winter aircraft icing storms during WISP90 and recommends the role of MWSRs in operational aircraft icing forecasts.

II. Description of Instruments and Techniques

Westwater and Kropfli[9] summarized many of the capabilities of WPL's instruments for measuring supercooled liquid water. Here we summarize the capabilities of those instruments used in WISP90.

Presented as Paper 91-0351 at the AIAA 29th Aerospace Sciences Meeting, Reno, NV, Jan. 7–10, 1991; received Jan. 11, 1991; revision received June 22, 1991; accepted for publication June 22, 1991.

*Wave Propagation Laboratory, 325 Broadway.

A. Dual-Channel Microwave Water Substance Radiometers

The dual-channel MWSRs measure downwelling radiation in the zenith direction at 20.6 and 31.65 GHz. The emission at 20.6 GHz is more sensitive to water vapor; 31.65 GHz is more sensitive to cloud liquid. From a simple retrieval algorithm,[2] precipitable water vapor V and integrated cloud liquid L are derived. The antenna beam width of the Stapleton MWSR is 2.5 deg; the beam widths of the Platteville and Elbert systems are 5.0 deg.

The microwave receivers are enclosed in shelters, internal temperatures of which are strictly controlled. The offset paraboloid antennas of the radiometers view, through a window that is nearly transparent to microwave radiation, a flat reflector located outside the instrument shelter. This reflector is oriented at 45 deg and thus reflects zenith radiation onto the offset paraboloid.

The current external reflector configuration can produce erroneous data when previously deposited ice on the reflector begins to melt, or when melting snow impacts on the surface. Stankov et al.[13] present quality control algorithms that rejected spurious radiometer data in post-time processing. This procedure could be used in real time, but a new experimental procedure to eliminate the problem at its source, i.e., prevention of ice and water buildup on the reflector, is suggested in Stankov et al.[13]

B. Infrared Cloud-Base Temperature Radiometer

To identify clouds and cloud types, we also operated two 10.6-μm infrared radiometers, one at Stapleton and one at Elbert. These instruments are housed in the same shelters as the MWSRs and have a vertical field of view of about 2.5 deg. Because of uncertainties in absolute calibration, the data are primarily qualitative. However, as shown in Section IV, there is excellent agreement in cloud identification between these infrared channels, the MWSRs, and the NWS ceilometer.

C. Wind Profilers and Radio Acoustic Sounding System

Wind-profiling radars[14] at Platteville, Erie, and Denver provided vertical profiles of the horizontal wind velocity and virtual temperature using the RASS technique.[11] The Platteville radar operates at a frequency of 49.8 MHz and uses four acoustic sources at frequencies near 110 Hz. This system covers the 3–6 km AGL height range, with a vertical resolution of 300 m. The Erie radar operates at 404.37 MHz and uses three acoustic sources near 900 Hz, covering the 2–4 km height range with a vertical resolution of 180 m. The Denver radar operates at 915 MHz and uses five acoustic sources near 2000 Hz providing the wind and temperature measurements with 150-m vertical resolution from 0.3 to 3.0 km AGL. All three radars are monostatic and use vertically-pointing radar and acoustic antenna beams when measuring temperature. During periods when aircraft icing conditions were expected, the RASSs at Denver and Erie measured vertical temperature profiles every 20 min.

D. Cloud-Top Computations

Remote observations of L from the MWSR, cloud-base height from the ceilometer, and cloud-base temperature from RASS were used with the moist adiabatic approximation method[10,13,15] to compute cloud depth and cloud-top height. Although moist adiabatic conditions are never truly reached in continental winter storms, this estimate of cloud-top height is a good first approximation[10,13] to the cloud top estimates in the typical shallow stratus encountered in winter storms east of the Rocky Mountains. This method can be generalized to cloud-type-dependent liquid water mixing ratio distributions.

III. Observations

There were 10 intensive observing periods during WISP90. The WPL instruments performed well during most of these periods. The quality control procedure used to eliminate erroneous data produced by melting ice on the MWSR reflector surface or by melting snow impacting on it is described by Stankov et al.,[13] and the quality control procedure applied to RASS data is described by Wuertz et al.[16] Here we present the results of three of those cases. They represent typical winter storm conditions for the Front Range region.

A. The "Valentine's Day Storm," February 12–15

Figure 1 shows an analysis of the NWS surface atmospheric observations (SAO) at 0000 UTC February 14. It shows the positions of a Pacific front and a trailing Arctic front farther north. An area of high pressure was moving southward from Canada over North Dakota, and a low-pressure center was over southern Utah and the Utah-Colorado Border. As a result, the surface flow was up the slope of the Front Range of the Colorado Rocky Mountains, and the air was saturated over a widespread region.

Figure 2a shows every third 20-min wind velocity profile observed with a 915 MHz wind profiler at Denver for the 64-h period starting at 1200 UTC February 12. The 5-min surface wind measurements at the Aurora mesonet station were used to linearly interpolate the winds from the ground to the first wind-profiler level. The first surface cold front was evident at ~2300 UTC February 12; the second front passed at ~0800 UTC February 13; and the third front passed at ~0700 UTC February 14. Figure 2b shows the time-height contour analysis of the N-S (V) wind velocity component. The zero line marks the shear zone between the northerly flow below and the southerly flow above. The northerly flow remained weak for the entire period, and the strongest wind speeds reached ~7 m s^{-1}. The wind speed in the southerly flow above reached ~30 m s^{-1}.

Figure 3 shows MWSR liquid water and water vapor time series at all three sites for the same 64 h shown in Fig. 2. There was a small increase in integrated liquid water (ILW) to ~0.2 mm at Platteville and Denver after the first front passed and a sharp jump to ~0.6 mm at all three sites after the second front passed at 0800 UTC February 13. ILW remained high for the next 24 h, averaging 0.4 mm at Platteville and Denver and 0.3 mm at Elbert. The maximum ILW of 0.8 mm was reached at 2200 UTC February 13 at Denver. During the remaining 28 h, the ILW remained elevated, averaging 0.15 mm at all three sites.

The time series in Fig. 4 represent the same time period as that in Figs. 2 and 3. Figure 4a shows time series of cloud-base height measured by the NWS lidar ceilometer at Denver, and cloud-top height estimated from the Denver radiometer ILW measurement using the moist adiabatic approximation,

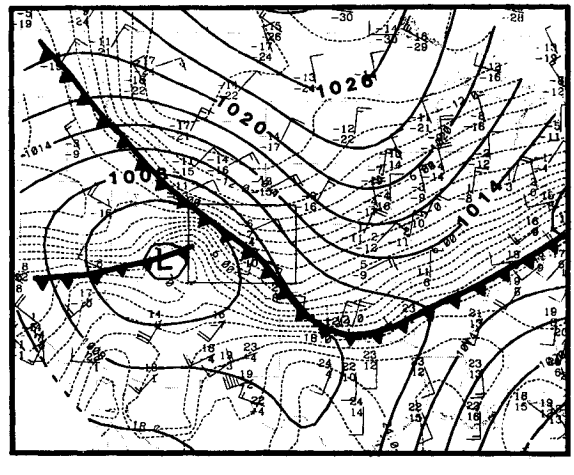

14-FEB-1990 0000 UTC

Fig. 1 Surface analysis of SAO data at 0000 UTC February 14. Temperature in °C (dashed lines), pressure in millibars (solid lines). Wind flag = 25 m s^{-1}, barb = 5 m s^{-1}, half barb = 2.5 m s^{-1}.

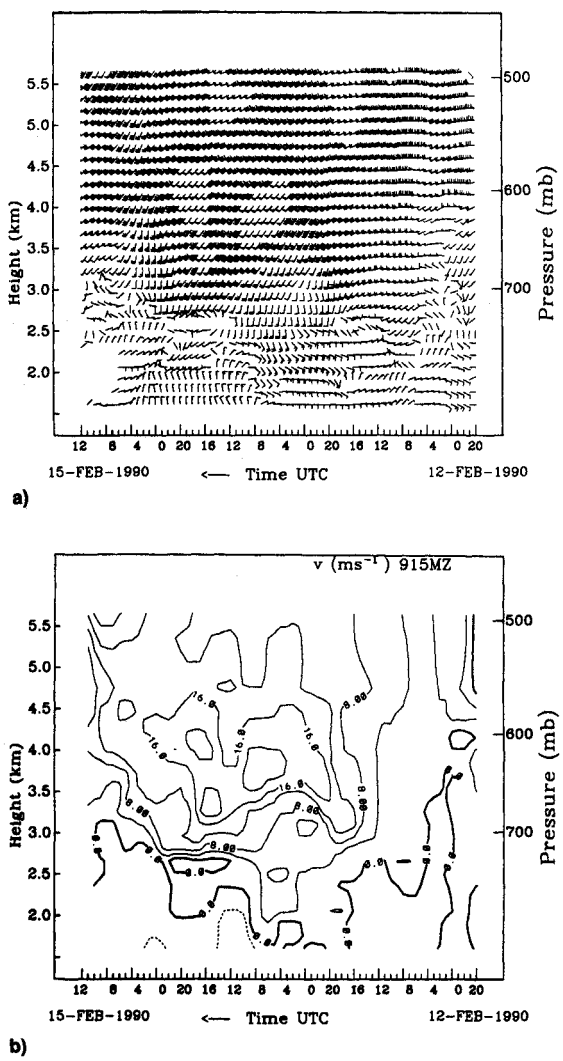

Fig. 2 a) Wind velocity 20-min profiles measured by the 915-MHz Stapleton wind profiler between 2000 UTC February 12 and 1200 UTC February 15. Wind flag = 25 m s^{-1}, barb = 5 m s^{-1}, half barb = 2.5 m s^{-1}; b) time-height analysis of (N-S) component of wind velocity V. Thin dashed lines are negative (northerly), thin solid lines are positive (southerly), and thick dashed line is zero. Ground level is at 1.611 km.

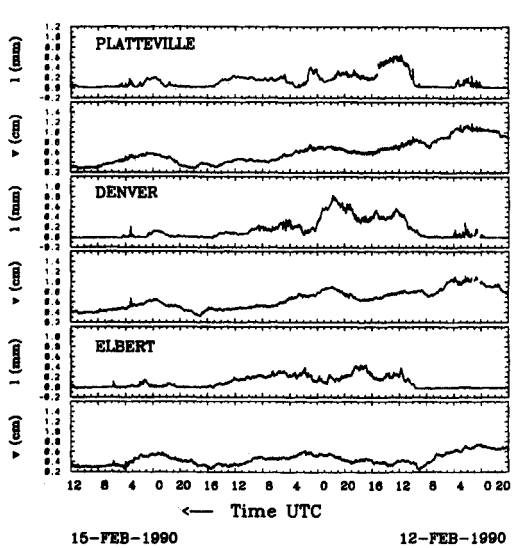

Fig. 3 Time series of liquid water content in millimeters and water vapor content in centimeters for 2000 UTC February 12 to 1200 UTC February 15 for Platteville, Denver, and Elbert.

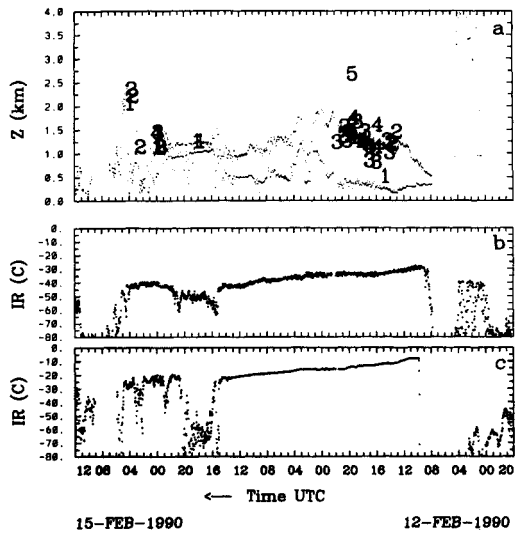

Fig. 4 Time series for 2000 UTC February 12 to 1200 UTC February 15; a) Denver lidar ceilometer cloud-base height measurement, cloud-top height computed using moist adiabatic approximation and aircraft icing severity at the height of PIREP, where 1 = light, 2 = light-to-moderate, 3 = moderate, 4 = moderate-to-severe and 5 = severe; b) infrared radiometer measurement of the cloud-base temperature at Denver; c) infrared radiometer measurement at Elbert.

ceilometer cloud-base measurement, and microwave radiometer measurement of the saturation vapor pressure at the cloud base.[10] The numbers in Fig. 4a represent the severity and altitude of aircraft icing reported by commercial pilots (PIREPS) in the Denver area. Figures 4b and 4c shows infrared radiometer time series for Denver and Elbert. Associated with the passage of the first front was a patch of high clouds evident in both the ceilometer and the infrared radiometer measurements. The observations on Fig. 4 show a sharp onset of low clouds and aircraft icing following the passage of the second front. The adiabatic cloud-top estimate was between 1.6 and 2.5 km AGL, which is in good agreement with the inversion height obtained from special radiosonde soundings.

Figure 5a shows the time-height analysis of combined temperature data from Denver and Platteville RASS in °C and repeats the cloud-base measurements and cloud-top estimates from Fig. 4a. Cooling associated with the first front is evident, but the surface temperatures are still about 10°C. After the second front passed at 0800 UTC February 13, the temperature dropped to below 0°C near the ground, and by 1100 UTC the entire temperature profile up to 500 mb was below 0°C. The cooling inside the frontal inversion continued, but the temperatures remained in the 0° to −15°C range. At 0700 UTC February 14, the third shallow cold front passed through the Front Range area, continuing the cooling inside the inversion layer to −20°C. However, the cloud-top temperatures remained warm at about −10°C as a result of the warm air advection at the 700 mb level. This provided excellent conditions for the presence of supercooled liquid water. Colder cloud-top temperatures may have nucleated higher numbers of ice crystals, which could have depleted the liquid in the cloud. Figure 5b shows the time-height analysis of the potential temperature (θ) computed from the Platteville and Denver RASS data. The stable layer associated with the surface cold front passages is clearly defined. The warm air advection at 700 mb level at 2000 UTC February 14 is shown as a wave inside the stably stratified layer. Figure 5c repeats the cloud-base and cloud-top estimate from Fig. 4a and shows the areas where the high vertical resolution Richardson number computed from RASS and wind-profiler data was below 2.5. Although the air above the cloud top is stably stratified, the Richardson number shows that the wind speeds of 15 m s^{-1} were sufficient to produce turbulent mixing and an additional aircraft hazard.

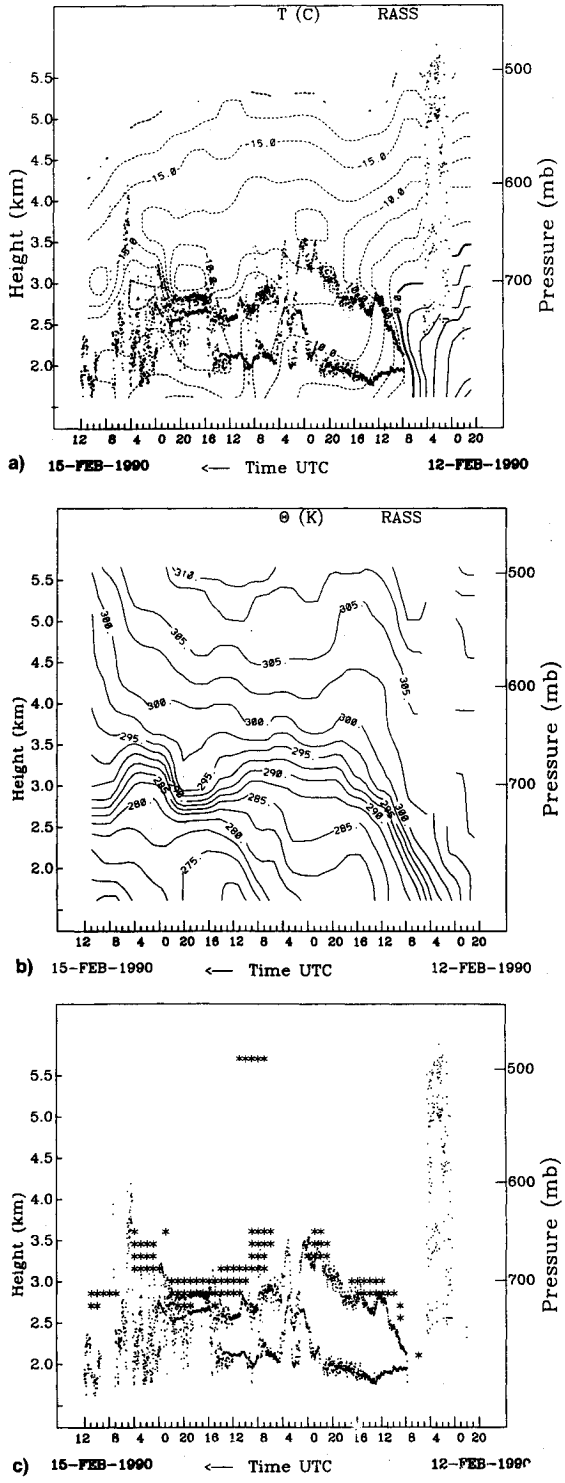

Fig. 5 a) Time-height analysis of temperature °(C), measured by the Stapleton and Platteville RASS and a cloud-base and cloud-top repeated from Fig. 4; b) time-height analysis $\theta(K)$, computed from temperature measurements in Fig. 5a; and c) areas where Ri $\leq$ 2.5 indicated by *, and the cloud-base and cloud-top repeated from Fig. 4a, for a period 2000 UTC February 12 to 1200 UTC February 15. Ground level is at 1.611 km.

B. February 27–28 Storm

Analysis of the SAO data for 2100 UTC February 27 shows a high-pressure center over South Dakota (Fig. 6) and a surface cold front extending from Idaho through Arkansas. The surface flow was northeasterly with the upslope component, and dewpoint temperatures were near saturation. Figure 7a shows every third 20-min horizontal wind velocity profile observed with the 915 MHz wind profiler at Denver for the 40-

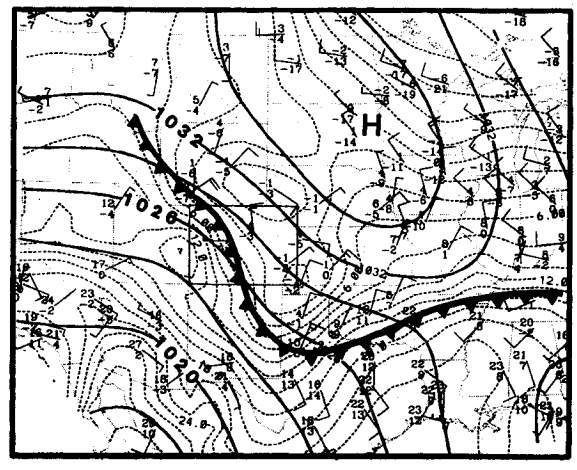

27-FEB-1990 2100 UTC

Fig. 6 Same as Fig. 1, but for 2100 UTC February 27.

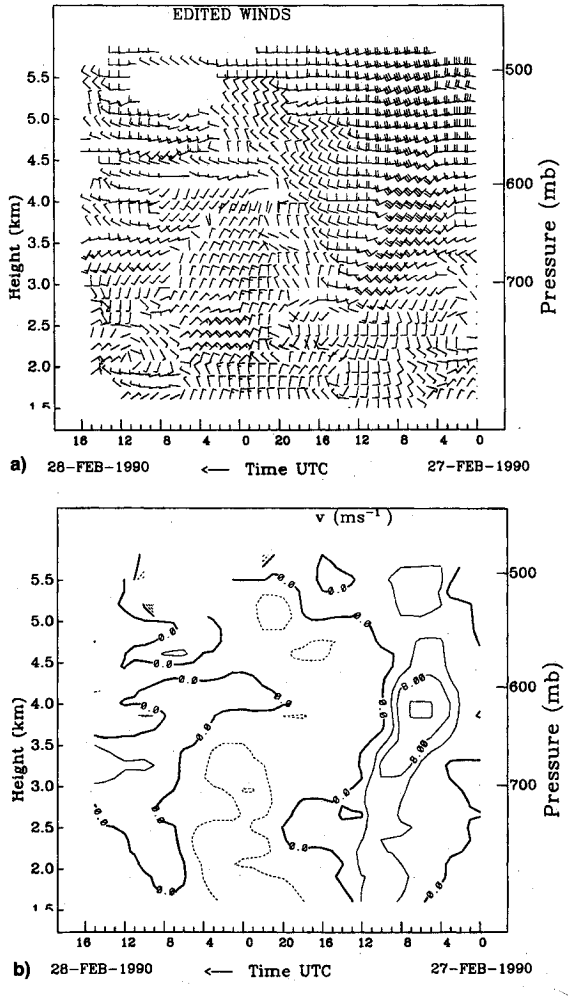

Fig. 7 Same as Fig. 2, but for 0000 UTC February 27 to 1600 UTC February 28.

h period starting at 0000 UTC February 27, and Fig. 7b shows the N-S wind component. Initially there was a 5-h period of weakly defined northerlies following the passage of a slow-moving surface cold front at 0000 UTC February 27. This northerly flow was followed by an 8-h period of weak southerly flow. At 1300 UTC February 27, however, there was a turn to northerly flow, which lasted for 15 h and reached speeds of ~8 m s^{-1} at 2100 UTC February 27 in a layer between the surface and 650 mb level. Liquid water measurements (Fig. 8) show an increase to 0.2 mm at 0400 UTC

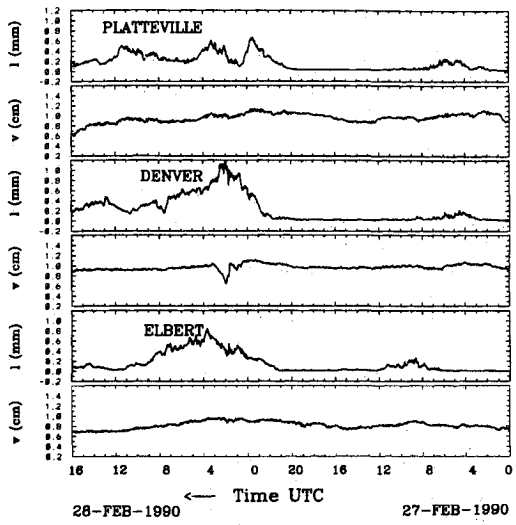

Fig. 8 Same as Fig. 3, but for 0000 UTC February 27 to 1600 UTC February 28.

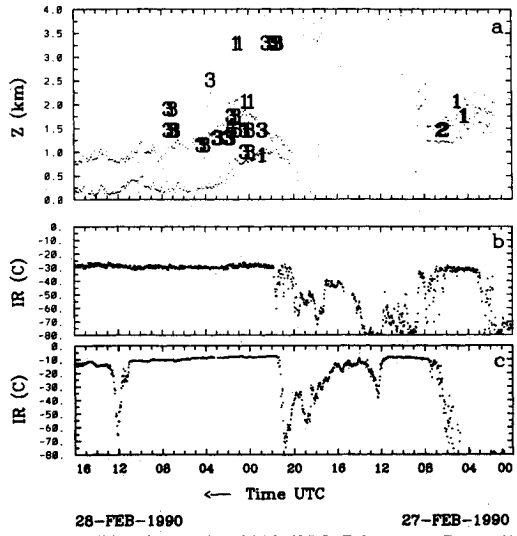

Fig. 9 Same as Fig. 4, but for 0000 UTC February 27 to 1600 UTC February 28.

February 27 associated with the front, but the increase was delayed by 4 h at Elbert. At 2100 UTC February 27, there was a new surge of cold air from north, and the ILW showed sharp increases to 1 mm at Denver, 0.8 mm at Elbert, and 0.6 mm at Platteville. Infrared radiometer data in Fig. 9 show the onset of low-level clouds after the frontal passage; the cloud onset at Elbert was 4 h later than at Denver. The onset was followed by a period of broken high clouds and a long period of persistent low-level clouds associated with the cold air surge at 2100 UTC February 27. Ceilometer cloud-base and cloud-depth measurements show similar behavior, although the PIREPS showed that aircraft icing was strongest following the second cold air surge. Note also that in the period from 0000 to 1800 UTC February 27, a large percentage of the clouds observed by the infrared radiometer and the ceilometer do not appear in the liquid signature observed by the MWSRs. Thus, the observed clouds did not contain liquid. A time-height analysis of combined Erie and Platteville RASS temperatures (Fig. 10a) shows the initial mild drop of temperature and then a sharp temperature drop at 2100 UTC February 27. Cloud-top and cloud-base estimates from Fig. 9a are repeated in Fig. 10a and coincide with the period of cold northerlies. Figures 10b and c show the potential temperature (θ) time-height analysis and the areas where the Richardson number was below 2.5. In this case the weak stable stratification allows for small Richardson numbers in spite of the weak winds (2.5 m s^{-1}).

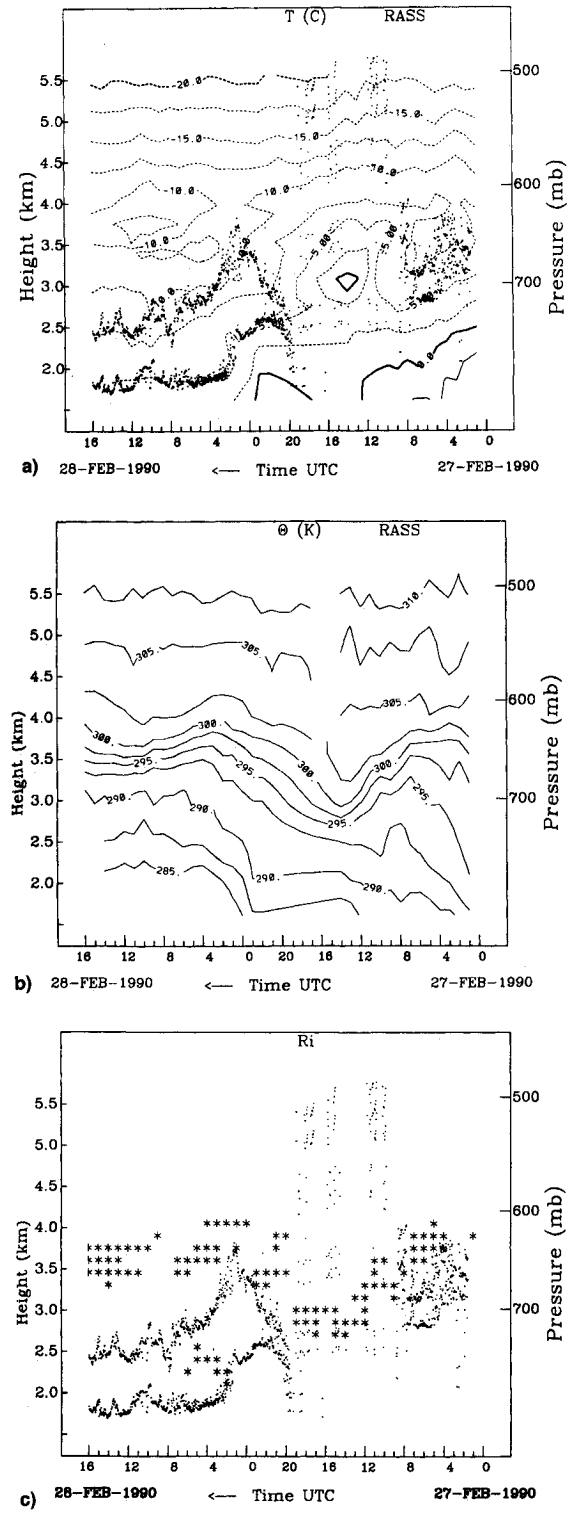

Fig. 10 Same as Fig. 5, but for 0000 UTC February 27 to 1600 UTC February 27.

C. March 22–24 Storm

The 0300 UTC March 23 SAO data analysis in Fig. 11 shows a cold front that just passed through Denver. The temperature behind the front was −8°C; in the warm air ahead of the front, it was 11°C. A high-pressure cell was over Montana, pushing the air southwestward toward the mountains. Figure 12 shows the onset of stronger northerlies, associated with the frontal passage, at 2300 UTC March 22 and a shear zone between the surface northerlies and the southerlies aloft. Liquid water (Fig. 13) jumped to 0.8 mm behind the front and remained at 0.4 mm on the average throughout the remaining

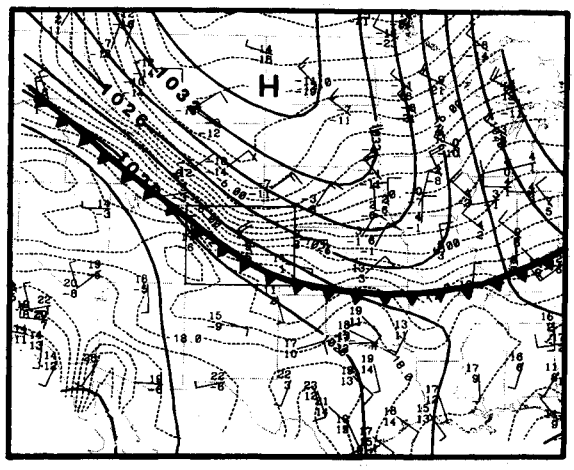

Fig. 11 Same as Fig. 1, but for 0300 UTC March 23.

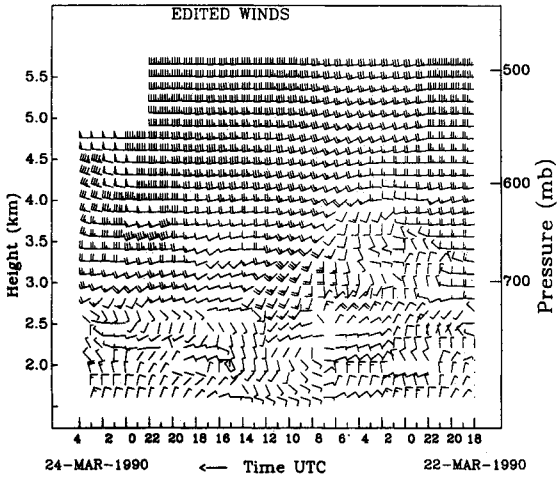

Fig. 12 Same as Fig. 2a, but for 1800 UTC March 22 to 0400 UTC March 24.

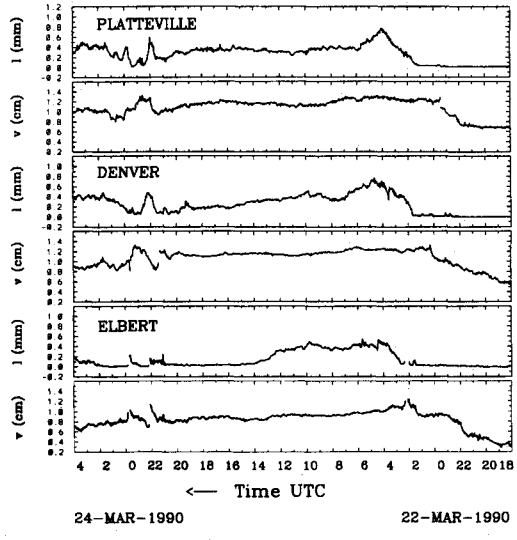

Fig. 13 Same as Fig. 3, but for 1800 UTC March 22 to 0400 UTC March 24.

26 h of this winter icing storm. Water vapor amounts started increasing 4–5 h before the frontal passage and remained at 0.8 cm. Infrared radiometers (Fig. 14) showed the onset of the front very sharply, indicating low clouds behind the front. The ceilometer at Denver had transmission problems for the first 24 h of the strom, but when the data were restored, they were consistent with those obtained with the infrared radi-

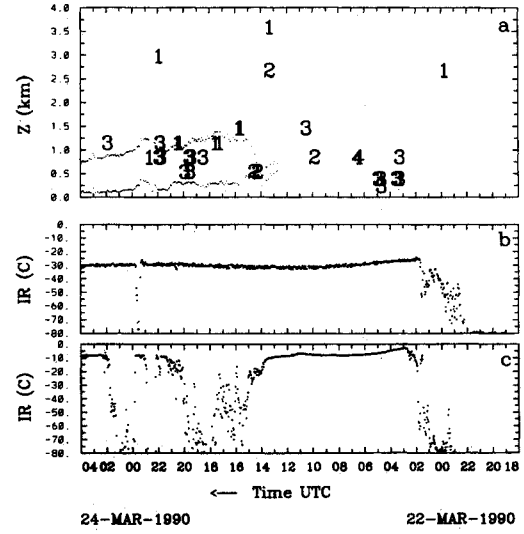

Fig. 14 Same as Fig. 4, but for 1800 UTC March 22 to 0400 UTC March 24.

ometers. PIREPS indicated aircraft icing of moderate severity after the temperature drop caused by the front. Figure 15a shows the time-height analysis of the combined Denver and Platteville RASS and the cloud-top and cloud-base estimates from Fig. 14. The temperature drop of about 20°C is evident with the frontal passage, as is the continual cooling behind it. A period of warm air advection at the 700 mb level after 1400 UTC March 23 increases the stable stratification (Fig. 15b) there. Figure 15c shows that the areas of low Richardson numbers are again above the cloud top where the southeasterlies were reaching 12 m s^{-1}. Thus even the mild conditions of this winter storm produces pockets of turbulence in the icing area.

IV. Applications of Remote-Sounding Data

A. Nowcasts and Real-Time Monitoring of Icing Conditions

Continuous measurements and unattended operation are inherent advantages of the remote sensors over the traditional NWS sampling with radiosondes. However, no single remote sensor is adequate for monitoring aircraft icing hazards. Appropriate combinations, however, can be very valuable.

Infrared and Ceilometer Data

As discussed in Section II, without absolute calibration, the infrared radiometer data were only of qualitative value. However, visual inspection of time series of these data, of ceilometer data, and of MWSR measurements of cloud liquid showed the infrared system to be a valuable indicator of sky cloud conditions. If the measured temperature was very cold (~80°C), skies were clear. If the data fluctuated wildly, over a 30°–40°C temperature range, ice clouds were generally indicated. Finally, if the readings were relatively warm (~ −10°C), then liquid clouds were present if also detected by the MWSR. Thus, although the infrared instrument is not a substitute for the quantitative ceilometer data, it has been useful in the general interpretation of MWSR data.

Ceilometer and RASS Data

Comparisons of the RASS temperature measurements from all three radar sites with nearby radiosonde temperature measurements (which were much less frequent) showed excellent agreement.[15] The combination of RASS and a ceilometer (or any method of deriving cloud-base height) can determine if the cloud-base temperature is below freezing. This combination cannot, however, determine if an observed cloud contains liquid.

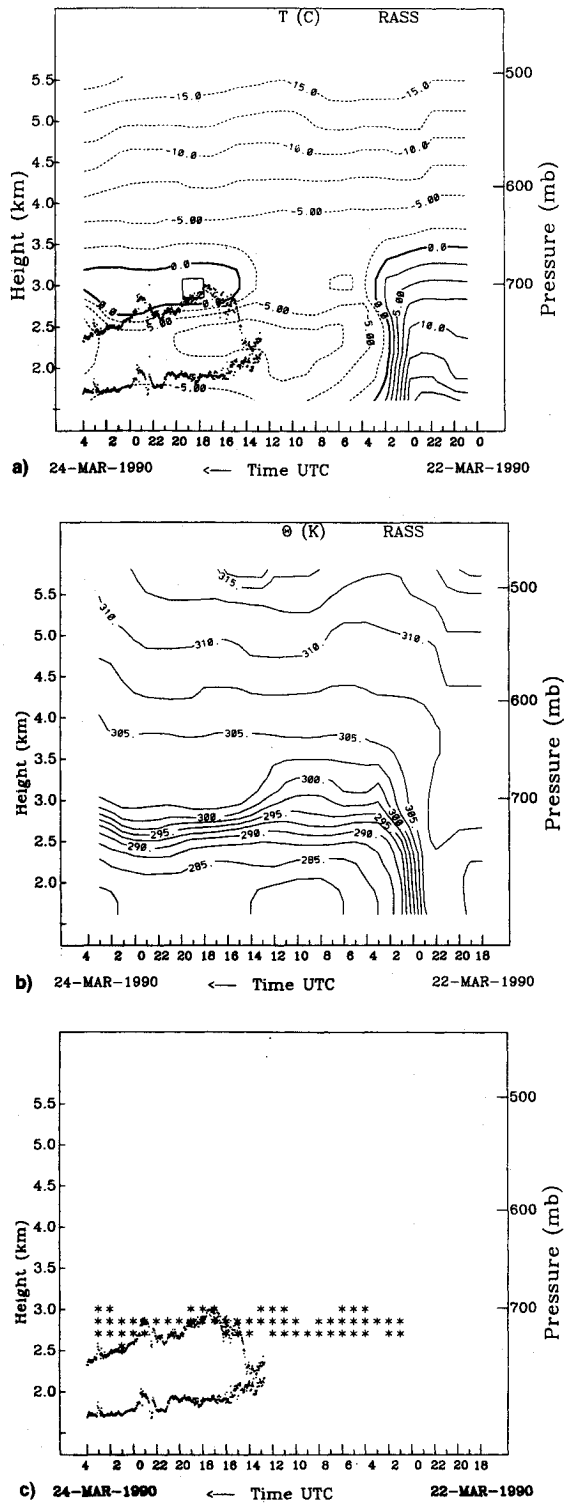

Fig. 15 Same as Fig. 5, but for 1800 UTC March 22 to 0400 UTC March 24.

MWSR, RASS, and Ceilometer

One must distinguish between two situations when combining measurements obtained using an MWSR, a RASS, and a ceilometer.

Case 1: Cloud-base temperature below freezing. If the MWSR indicates that a cloud contains liquid, and the ceilometer and RASS indicate that the cloud-base temperature is below freezing, then the observed liquid is supercooled. The data discussed in Section III provide excellent confirmation of this technique. In addition, if the adiabatic approximation is used, then an effective liquid cloud-top height can be derived. The examples presented in Section III qualitatively agree with this technique. The technique could be improved by using additional information to adjust the liquid water to allow for entrainment or depletion by ice in a cloud-top-adjusted parameterization scheme.

Case 2: Cloud-base temperature above freezing. If the cloud-base temperature is above freezing, the combined data cannot unambiguously determine if observed liquid is supercooled. However, the RASS and the ceilometer can measure the thickness of the region between the cloud base and the 0° isotherm and, with the adiabatic assumption, be used to estimate the liquid amount in the portion of the cloud that is above freezing. If this amount is substantialy less than the observed total liquid, then there is confidence that supercooled liquid exists. None of the three cases reported here had a cloud-base temperature above freezing.

B. Forecast Validation

RASS

Time series of vertical profiles of temperature from RASS could be useful in temperature forecast validation and storm diagnostics.

Ceilometer

It is self-evident that time series of cloud-base height could be used to validate some aspects of cloud liquid forecasts. Cloud-base information is important for knowledge of icing altitudes. The ceilometer data, however, have little usefulness for determining cloud depth.

MWSR

Calculations of the vertical profiles of cloud liquid densty ρ^1 could be integrated and compared with the integrated liquid measured by the radiometers. Time-height cross sections of forecast ρ^1 could be compared with radiometer data to study storm evolution.

MWSR, BASS, and Ceilometer

Data from this combination of sensors provide an estimate of SLW that could be compared with a forecast. With reasonable assumptions, an estimate of profiles of ρ^1 could be derived. In addition, if surface measurements of water vapor density were available, this combination could also provide a reasonable estimate of water vapor profiles.

C. Forecasts

RASS

Since RASS measures virtual temperature of the air, a combination of microwave radiometer humidity measurements by retreival techniques and RASS temperature measurements should be used in numerical prediction models for all scales of motions. RASS temperature measurements can and should be incorporated into forecast models in real time.

MWSR

Precipitable water vapor measurements from MWSRs have been used with a variational technique to constrain satellite determinations of vapor.[17] The precipitable vapor can also be combined with a model to derive vapor profiles and to adjust and constrain the model. Time measurements of liquid water could be used for model initialization, at least at the discrete points of a limited network, as well as in subsequent "nudging."

V. Summary

Finally, the preliminary success of the combination of instruments to identify vertical regions of SLW was impressive. We feel that both RASS and MWSR should be considered for national deployment.

During WISP91, January 15 to March 31, 1991, WPL deployed a variety of remote sensors. These sensors included:

a network of 4 MWSRs, RASS temperature measurements using 915, 405, and 50 MHz wind profiling radars, ceilometers, and a new "mini-Profiler."[18] The suggested improvements[13] in antenna maintenance have been implemented on the radiometers and their performances carefully monitored during WISP91 snowfall conditions. Thus a variety of systems were available for unattended deployment during the 1991 winter storm season. The success of combined sensor products in deriving the height range of supercooled liquid again proved their usefulness for icing nowcasting.

The WPL steerable radiometer[2] was also used in a scanning mode to extend the horizontal coverage beyond that of a zenith-viewing instrument. During a portion of WISP91, both the steerable radiometer and a dual-wavelength radar[9] were used to study the possibility of determining profiles of cloud liquid.

Acknowledgments

The FAA funded this project under DTAF01-90-Z-02005. The Thermodynamic Profiling group and the Wind Profiler Research group of WPL spent many extra hours ensuring continual data flow from the instrument sites. This study would not have been possible without Richard Beeler, Duane Hazen, Mark Jacobsen, Bill Madsen, Martin Decker,and Tom Stermitz, who provided radiometer data, and Peter May, Ken Moran, Dick Strauch, and Dave Merritt, who provided the RASS data. Brooks Martner provided insightful comments on the manuscript, and Melvyn Shapiro suggested an improvement on Richardson number calculation. Wayne Sand, Marcia Politovich, and Roy Rasmussen of NCAR RAP project operations conducted a well-organized and well-executed scientific experiment. Kim Elmore from NCAR RAP provided aircraft data and deserves commendation for setting up the radio-based communications link to the remote Elbert site.

References

[1]Westwater, E. R., "Ground-Based Microwave Remote Sensing of Meteorological Variables," *Atmospheric Remote Sensing by Microwave Radiometers*, Wiley, New York, 1990, Chap. 4.

[2]Hogg, D. C., Guiraud, F. O., Snider, J. B., Decker, M. T., and Westwater, E. R., "A Steerable Dual-Channel Microwave Radiometer for Measurement of Water Vapor and Liquid in the Troposphere,' *Journal of Applied Meteorology*, Vol. 22, No. 5, 1983, pp. 789–806.

[3]Rauber, R. M., and Grant, L. O., "The Characteristics and Distribution of Cloud Water over Mountains of Northern Colorado during Winterstorms. Part II: Spatial Distribution and Microphysical Characteristics," *Journal of Applied Meteorology*, Vol. 25, No. 4, 1986, pp. 489–504.

[4]Reynolds, D. W., "A Report on Winter Snowpack Augmentation," *Bulletin of American Meteorological Society*, Vol. 69, No. 11, 1988, pp. 1290–1299.

[5]Uttal, T., Snider, J. B., Kropfli, R. A., and Orr, B. W, "A Remote Sensing Method of Measuring Atmospheric Vapor Fluxes: Application to Winter Mountain Storms," *Journal of Applied Meteorology*, Vol. 29, No. 1, 1990, pp. 22–34.

[6]Hogg, D. C., Decker, M. T., Guiraud, F. O., Earnshaw, K. B., Merritt, D. A., Moran, K. P., Sweezy, W. B., Strauch, R. G., Westwater, E. R., and Little C. G., "An Automatic Profiler of the Temperature, Wind and Humidity in the Troposphere," *Journal of Applied Meteorology*, Vol. 22, No. 5, 1983, pp. 807–831.

[7]Hogg, D. C., Guiraud, F. O., and Burton, E. B., "Simultaneous Observation of Cool Cloud Liquid by Ground-Based Microwave Radiometry and Icing of Aircraft, *Journal of Applied Meteorology*, Vol. 19, No. 7, 1980, pp. 893–895.

[8]Popa Fotino, I. A., Schroeder, J. A., and Decker, M. T., "Ground-Based Detection of Aircraft Icing Conditions Using Microwave Radiometers," *Institute of Electrical and Electronic Engineers Transactions on Geosci. Remote Sens.*, GE-24, 1986, pp. 975–982.

[9]Westwater, E. R., and Kropfli, R. A., "Remote Sensing Techniques of the Wave Propagation Laboratory for Measurement of Supercooled Liquid Water: Applications to Aircraft Icing," National Oceanic and Atmospheric Administration/Environmental Resource Lab., NOAA TM ERL WPL-163, Boulder, CO, 1989.

[10]Stankov, B. B., and Bedard, A. J. "Remote Sensing Observations of Winter Aircraft Icing Conditions: A Case Study." *AIAA Journal* (to be published).

[11]May, P. T., Strauch, R. G., and Moran, K. P., "The Altitude Coverage of Temperature Measurements Using RASS with Wind Profiler Radars," *Geophysical Research Letters*, Vol. 15, No. 12, 1988, pp. 1381–1384.

[12]Rasmussen, R., and Politovich, M. K., Winter Icing Storms Project (WISP), *Scientific Overview*, National Center for Atmospheric Research, Boulder, CO, 1990.

[13]Stankov, B. B., Westwater, E. R., Snider, J. B., and Weber, R. L., "Remote Sensor Observations During WISP90: The Use of Microwave Radiometers, RASS, and Ceilometers for Detection of Aircraft Icing Conditions." National Oceanic and Atmospheric Administration/Environmental Research Lab., NOAA TM ERL WPL-187, Boulder, CO, 1990.

[14]Larsen, M. F., and Rottger, J. VHF and UHF Doppler Radars as Tools for Synoptic Research. *Bulletin of the American Meteorological Society*, Vol. 63, No. 9, 1982, pp. 996–1008.

[15]Albrecht, B. A., Fairall, C. W., Thomson, D. W., White, A. B., Snider, J. B., and Schubert, W. H. "Surface-Based Remote Sensing of the Observed and Adiabatic Liquid Water Content of Stratocumulus Clouds." *Geophysical Research Letters*, Vol. 17, 1990, pp. 89–92.

[16]Wuertz, D. B., Webber, B. L., Strauch, R. G., Moran, K. P., Merritt, D. A., and Goldstein, M. H., "RASS Temperature Measurements 1990 Winter Icing Experiment." National Oceanic and Atmospheric Administration/Environmental Research Lab., NOAA TM ERL WPL-190, Boulder, CO, 1990.

[17]Birkenheuer, D., "An Algorithm for Operational Water Vapor Analyses Integrating GOES and Dual Channel Microwave Radiometer Data on the Local Scale," *Journal of Applied Meterology*, Vol. 30, No. 6, June 1991.

[18]Neff, W., Jordan, J., Gaynor, J., Wolfe, D., Ecklund, W., Carter, D., and Gage, K., "The Use of 915 MHz Wind Profilers in Complex Terrain and Regional Air Quality Studies," Preprint Vol.: Seventh Joint Conf. on Applications of Air Pollution Meteorology with American Meterological Society, New Orleans, LA, Jan. 13–18, 1991. American Meteorological Society, Boston, MA.